Available online at BCREC website: https://bcrec.id

Bulletin of Chemical Reaction Engineering & Catalysis, 18 (4) 2023, 724-735

Research Article

MOF-199 and Ni-BTC: Synthesis, Physicochemical Properties, and Catalytic Activity in Oxidation of 5-Hydroxymethylfurfural

Idra Herlina[1,2,3], Yuni Krisyuningsih Krisnandi[1,2,*], Muhammad Ridwan[1]

[1]Department of Chemistry, Faculty of Mathematics and Natural Science, Universitas Indonesia, Depok 16424, Indonesia.
[2]Solid Inorganic Framework Laboratory, Department of Chemistry, Faculty of Mathematics and Natural Science (FMIPA), Universitas Indonesia; Depok 16424, Indonesia.
[3]Department of Chemistry, Institut Teknologi Sumatera, Terusan Ryacudu, Jati Agung, Lampung 35365, Indonesia.

Received: 20th October 2023; Revised: 6th December 2023; Accepted: 7th December 2023
Available online: 9th December 2023; Published regularly: December 2023

Abstract

Platform chemical 2,5-furandicarboxylic acid (FDCA) has potential applications to replace petroleum-based chemicals. Metal Organic Framework (MOF) can be used as a catalyst to oxidize 5-hydroxymethylfurfural (HMF), producing FDCA. MOF-199 and Ni-BTC were synthesized using solvothermal method with trimesic acid (benzene 1,3,5-tricarboxylic acid/H_3BTC) as a linker and Cu or Ni as a metal nod. The physical and chemical properties of catalysts were discovered through characterization using X-ray Diffraction (XRD), Fourier Transform Infra Red (FT-IR), Thermogravimetric Analysis (TGA), Scanning Electron Microscopy - Energy Dispersive X-ray (SEM-EDX), and Ammonia Temperature-programmed Desorption (NH_3-TPD). FDCA and its intermediate compounds were produced by converting HMF to FDCA in a small glass batch reactor. The yields of products were then determined by High-Performance Liquid Chromatography (HPLC). HPLC results indicated that there was no DFF (2,5-diformylfuran) signal, indicating that FDCA was formed by FFCA (5-formylfuroic acid) and HMFCA (5-hydroxymethylfuroic acid) formation reaction pathway. The maximum conversion (71%) was obtained using Ni-BTC as a catalyst at 130 °C for 5 h, with FDCA yield of 61.8%.

Copyright © 2023 by Authors, Published by BCREC Group. This is an open access article under the CC BY-SA License (https://creativecommons.org/licenses/by-sa/4.0).

Keywords: MOF-199; Ni-BTC; 5-hydroxymethylfurfural; 2,5-furandicarboxylic acid

How to Cite: I. Herlina, Y.K. Krisnandi, M. Ridwan (2024). MOF-199 and Ni-BTC: Synthesis, Physicochemical Properties, and Catalytic Activity in Oxidation of 5-Hydroxymethylfurfural. *Bulletin of Chemical Reaction Engineering & Catalysis*, 18 (4), 724-735 (doi: 10.9767/bcrec.20060)

Permalink/DOI: https://doi.org/10.9767/bcrec.20060 ;
Supporting Information (SI): https://journal.bcrec.id/index.php/bcrec/article/downloadSuppFile/20060/5101

1. Introduction

Biomass resources can be converted into clean energy through a variety of technologies. Biomass consists of wastewater, municipal waste, animal residues, industrial residues, forestry crops and residues, and agricultural crops and residues [1]. An example of agricultural residues that can be used as a renewable energy source is rice husks. The main components of rice husks are lignin and cellulose, with trace amounts of water, ash, and extractive matter [2]. Cellulose is a polysaccharide that can be converted into glucose through hydrolysis reaction. The decomposition of glucose will produce

* Corresponding Author.
Email: yuni.krisnandi@sci.ui.ac.id (Y.K. Krisnandi);
Telp: +62-21-7270027, Fax: +62-21-7270012

5-hydroxymethylfurfural (HMF). Furthermore, HMF can be converted into other platform compounds, such as 2,5-diformylfuran (DFF), 2,5-bis(hydroxymethyl)-furan (BHMF), levulinic acid, 2,5-dimethylfuran (DMF), and 2,5-furandicarboxylic acid (FDCA) [3].

FDCA (2,5-furandicarboxylic acid) is one of 12 priority chemicals [4]. FDCA is multifunctional due to its cyclic structure and two carboxyl groups [5]. The production of polyester, polyurethane, and polyamide is one of the potential uses for FDCA [6–8]. Oxygen or peroxide is typically used as the oxidizing agent in the oxidation reaction over heterogeneous catalysts, such as MnO_2 [9], Au/C [10], Pd-Bi-Te/C [11], Pt/CeO_2 [12], and Cr_2O_3/CeO_2 [13], to produce FDCA from 5-hydroxymethylfurfural (HMF). According to Stöcker [14], the existence of porous materials with practical accessibility to acidic, basic, or metal sites with a large surface area can enhance the performance of metals as catalysts. In this study, the catalyst is based on a metal-organic framework with transition metal oxides (Cu and Ni). It has not been widely reported that MOF can be used as a catalyst to oxidize HMF to FDCA.

MOF-type catalysts are porous coordination polymers consisting of a metal core and organic ligands (linkers) which can be controlled by variations in ligands and metals, functional groups, and pores [15]; so that it can be modified according to the required functionality for the biomass reaction [16]. In this study, MOF synthesis goes through the solvotermal method. The linker is trimesic acid (benzene 1,3,5-tricarboxylic acid/H_3BTC) to produce MOF with the HKUST-1 (Hong Kong University of Science and Technology) type, also known as MOF-199 where the BTC ligand coordinate metal ions in the cubic lattice (Fm-3m) [17]. MOF-199 is known to have interconversion of metals in different oxidation states, resistance to toxic intermediates, and extraordinary stability in methanol oxidation in alkaline media [18] making it an attractive candidate catalyst in the oxidation reaction of HMF to FDCA. Thus, in this study, we observed the physicochemical properties of catalysts. Furthermore, effectiveness of MOF-199 made of Cu metal will be evaluated in comparison to MOF made of Ni metal and how reaction time affected the final product. Catalytic activity test using a vial bottle with a stainless-steel vial holder which is immersed in an oil bath. The supply of oxygen which supports the oxidation reaction is provided by hydrogen peroxide. The reaction was carried out at 130 °C.

2. Materials and Methods

2.1 Materials

The materials used in the experiments included nickel(II) nitrate hexahydrate ($Ni(NO_3)_2.6H_2O$, ≥99.5%), copper(II) nitrate trihydrate ($Cu(NO_3)_2.3H_2O$, ≥99.5%), methanol (≥99.8%), ethanol (≥99.5%), N,N-dimethyl formamide (≥99.8%), hydrogen peroxide (H_2O_2, 30%), sulfuric acid (H_2SO_4, 96%), potassium carbonate (K_2CO_3, ≥99%) were purchased from Merck (Germany). Benzene 1,3,5-tricarboxylic acid (H_3BTC, 95%), 5-hydroxymethylfurfural (HMF, ≥99%), 2,5-furandicarboxylic acid (FDCA, 97%), 5-hydroxymethylfuroic acid (HMFCA, ≥95%), 5-formylfuroic acid (FFCA, 97%), and 2,5-diformylfuran (DFF, 97%) were purchased from Sigma Aldrich (US) and directly used without purification.

2.2 Synthesis of MOF-199 and Ni-BTC

Synthesis of MOF-199 and Ni-BTC through the solvothermal method refers to [19–21]. For MOF-199, 2.07 grams of $Cu(NO_3)_2.3H_2O$ was dissolved in 15 mL of distilled water, and 1 gram of H_3BTC was dissolved in 30 mL of a mixture of ethanol and DMF (1:1). For Ni-BTC, 2.5 grams of $Ni(NO_3)_2.6H_2O$ dissolved in 15 mL of distilled water. Separately, 1.05 grams of H_3BTC was dissolved in 20 mL of DMF. The homogeneous mixture was then transferred into a teflon-lined autoclave and heated at 100 °C for 10 h for MOF-199 and 160 °C for 48 h for Ni-BTC. After the reaction was complete, the autoclave was slowly cooled to room temperature. The solid formed was filtered, washed thrice with solvent, and dried at 65 °C for 24 h.

2.3 Characterization of Catalysts

FT-IR analysis was carried out using an Alpha-Bruker and XRD was carried out using a PANalytical XPert PRO 2318 diffractometer with Cu-Kα radiation (λ =1.54184 Å) as the incident beam. TGA was conducted using Perkin Elmer 4000, sample mass in the range 4-5 mg in a nitrogen atmosphere (flow rate of 20 mL/min) with a constant heating rate of 10 °C/min and at temperature of 25-400 °C. SEM-EDS was conducted using a FE-SEM JIB-4610F microscope equipped with a Schottky electron gun robe current (200nA), electron backscatter diffraction (EBSD) to perform crystallographic characterization, and cathodoluminescence (CLD). Moreover, to determine the surface area of samples used Quantachrome Quadrasorb-Evo surface area and pore size analyzer. The Micrometric Chemisorb

Copyright © 2023, ISSN 1978-2993

2750 device was used to analyze the properties of acidity strength. Before NH_3 adsorption, 0.05 g sample was pre-treated by heating it for 60 min at 350 °C for 60 min under He gas (inert). This was followed by 30 min of NH_3 adsorption at 100 °C using 5% NH_3 in He (v/v), then purged with helium gas (inert) at the same temperature, for 30 min. After that, NH_3 desorption was conducted at 100–400 °C with a ramp rate of 10 °C/min. It was then maintained at 400 °C for 15 min at a total gas flow rate of 40 mL/min.

2.4 Catalytic Activity Test

In a typical reaction, a 20 mL vial containing 0.025 g of catalyst, 0.25 g of HMF, 5 mL of 2% H_2O_2, 0.75 g of K_2CO_3, and 5 mL of water were sealed, placed into stainless steel vial holder, and submerged in an oil bath. The mixture was stirred for 1-5 h at 130 °C. HMF and its derivatives were separated from the catalyst and then were analyzed with HPLC PG LC210 with C18 column and UV detector at 25 °C. The mobile phase was a mixture of 5 mM aqueous H_2SO_4 and methanol (9:1) with a 1 mL/min flow rate. HMF conversion, FDCA yield, and catalyst selectivity were calculated using the standard calibration curve and determined using following equations:

$$Conversion\ (\%) = \frac{C_0 - C_t}{C_0} \times 100 \quad (1)$$

$$Yield\ (\%) = \frac{C_{FDCA} \times V}{m_{HMF}} \times 100 \quad (2)$$

$$Selectivity\ (\%) = \frac{Yield\ (\%)}{Conversion\ (\%)} \times 100 \quad (3)$$

where, C_0 is the initial concentration of HMF (mg/L), C_t is the concentration of HMF after reaction (mg/L), C_{FDCA} is the FDCA concentration (mg/L), V is the volume of solution (L), m_{HMF} is the mass of HMF (mg).

3. Results and Discussion

3.1 Catalyst Characterization

The synthesis process of MOF-199 and Ni-BTC is shown in Figure 1. The as-synthesized MOF-199 crystal is blue, while Ni-BTC is green. The synthesis was carried out by the solvothermal method using a mixture of ethanol, DMF, and water as solvent. The MOF dimensions are strongly influenced by the solvent used. Ediati *et al.* [22] observed the effect of the ethanol and DMF solvents ratio on the physical properties of MOF-199 crystals. The effect of DMF on MOF-199 synthesis shows that the smaller the volume of DMF used, the smaller the MOF-199 crystals produced. The presence of DMF supports the formation of more and larger crystals, while ethanol and

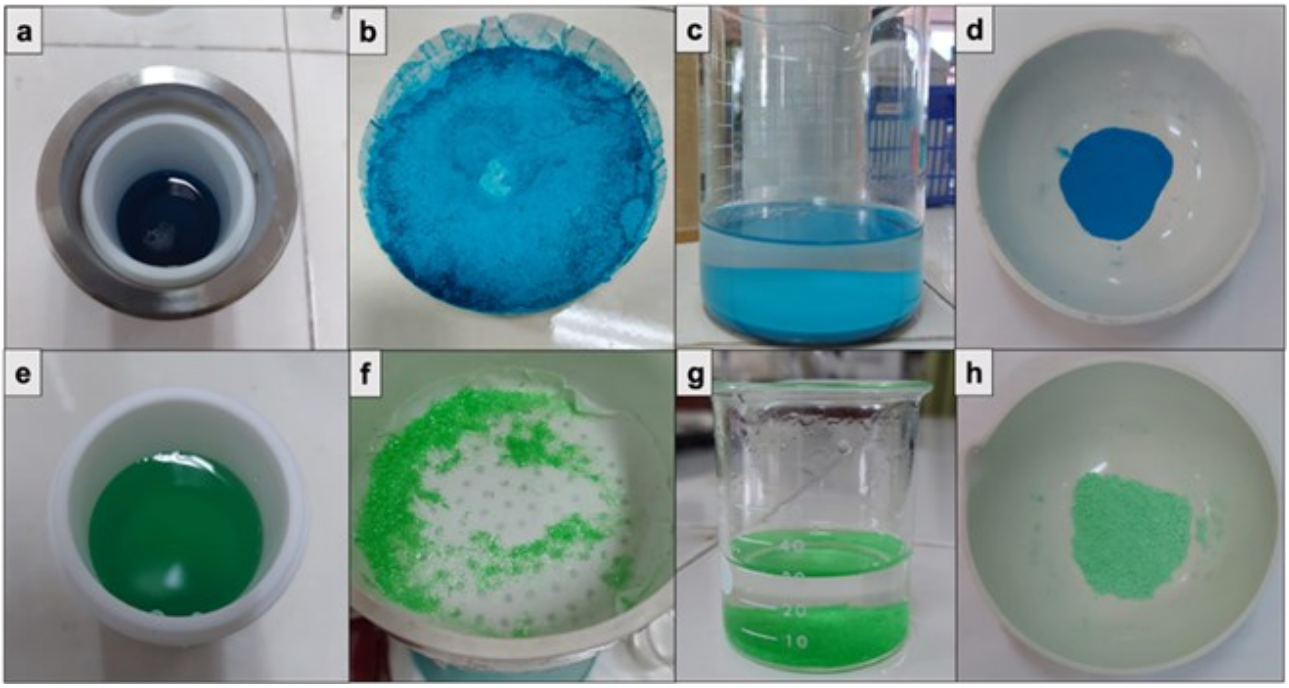

Figure 1. Synthesis process of MOF-199 (a-d) and Ni-BTC (e-h): solvothermal reaction in teflon-lined stainless steel (a and e), filtration (b and f), washing/solvent exchange (c and g), as-synthesized MOF (d and h).

Copyright © 2023, ISSN 1978-2993

water make the crystals more consistent. MOF-199, which has the best heat resistance and consistent crystals, is provided by a mixture of ethanol: DMF solvent at a ratio of 1:1. Therefore, the solvent ethanol: DMF was used in a ratio of 1:1 in this study.

The IR spectra of MOF-199 are shown in Figure 2(a), which shows a peak at 750 cm^{-1} corresponding to the substitution of Cu metal in the benzene group. The band at 1094 cm^{-1} corresponds to the CO–Cu loading of the MOF. The absorption at a wavelength of 1450–1360 cm^{-1} indicates the presence of aromatic C=C bonds and vibrations of carboxyl groups in BTC. The absorption at wavenumber 1650-1600 cm^{-1} indicates the C=O (carbonyl) group, and the broadband at wavenumber 3500 cm^{-1} indicates the presence of a physically bonded OH group from H_2O. This is confirmed by the presence of absorption at wavenumber 1300 cm^{-1}, indicating the presence of a single C–O bond in the carboxylic acid, and by the band at 1617 cm^{-1}, indicating H–O–H vibrations of water. Based on the results of FTIR analysis, it is known that HKUST-1 crystals formed due to the typical absorption that occurs in the four crystals according to the reference [22–24]. IR spectra of Ni-BTC shows identical spectra with absorption bands at 1438 cm^{-1}, 1562 cm^{-1}, and 1625 cm^{-1}. The bands show a similar IR absorption pattern to the Ni ion-coordinated COO groups in the region 1650-1350 cm^{-1} [26] and the vibrations of C–N and CN–CHO at 1055 cm^{-1} and 932 cm^{-1}. This shows the presence of Ni coordinating with the DMF molecule [27] and at 720 cm^{-1}, a typical Ni–O band.

The acidic properties of MOF-199 and Ni-BTC were measured using ammonia adsorption (NH_3-TPD), shown in Figure 2(b). Basically, the higher the desorption temperature, the

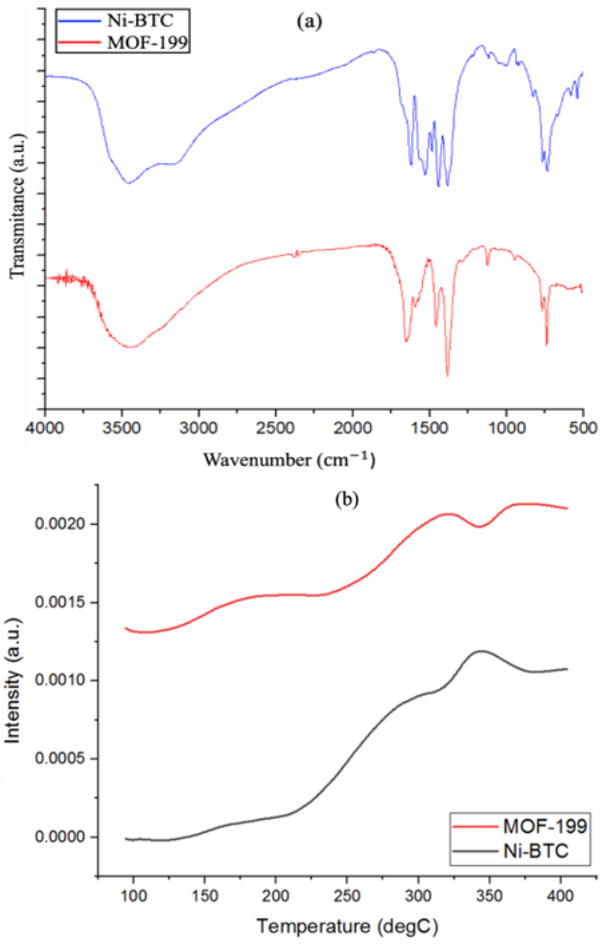

Figure 2. IR spectra (a) and NH_3-TPD curve (b) of MOF-199 and Ni-BTC.

Table 1. Acid amount in MOF-199 and Ni-BTC.

Catalyst	Acid Amount (mmol/g)
MOF-199	0.086
Ni-BTC	0.1084

**The acid content is determined by NH_3-TPD profile*

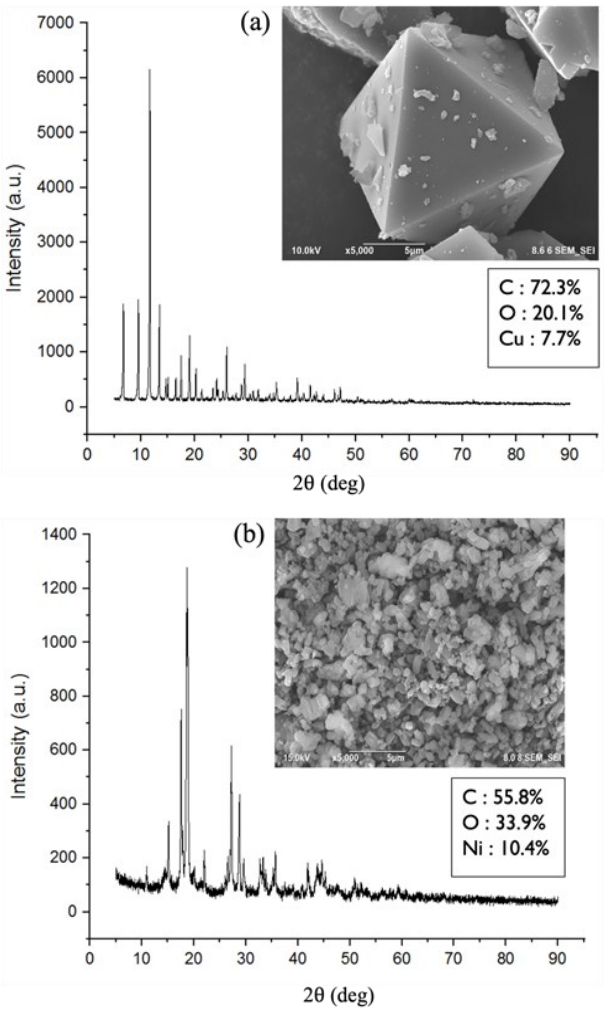

Figure 3. Diffractogram, SEM image, and elemental composition of (a) MOF-199 and (b) Ni-BTC.

Copyright © 2023, ISSN 1978-2993

stronger the acidity [28]. It can be seen from the MOF-199 curve (Figure 2(b)) that three main weak peaks appear at around 180, 320, and 370 °C, while for Ni-BTC they appear at around 170, 280, and 330 °C.

Table 1 shows the NH_3-TPD measurement results of the acid amount in MOF-199 and Ni-BTC is 0.086 and 0.1084 (mmol/g), respectively. Therefore, Ni-BTC is known to be more acidic than MOF-199. In addition to having a stronger Lewis acid, the MOF structure has more Ni coordinated than Cu (Figure 3). Because of this, Ni-BTC contains more acid than MOF-199 does. Nevertheless, it should be noted that the high temperature of TPD pretreatment (350 °C) allows damage to the MOF structure. This is also supported by DTG data (Figure 4), that the decomposition of MOF-199 and Ni-BTC at temperatures around 350 and 450 °C, respectively. However, Gao *et al.* [29] shows that the analysis results of NH_3-TPD MOF-199 at a high pretreatment temperature can be used to compare the acidity of MOF.

Figure 3(a) shows the diffractogram of MOF-199. Based on previous studies [30–32] the typical peak that occurs and indicates that HKUST-1 crystals have formed is at 2θ = 9.5°; 11.6°; and 13.4°, with the 11.6° peak having the highest intensity. Clear and sharp peaks indicate good crystallinity. All diffraction peaks correspond to the standard pattern. The synthesized sample was phase pure, as no apparent peaks of impurities were observed [33].

The Ni-BTC diffractogram (Figure 3(b)) is similar to the previously synthesized Ni-BTC [20]. The peaks at 2θ = 10°; 15°; and 27.5° are due to the presence of nickel oxide and the formation of hydroxide. Peaks at 2θ = 35°; 42°; and 51° indicate the presence of nickel.

Field Emission Scanning Electron Microscopy (FE-SEM) was used to investigate morphology, crystallinity, and microstructure of catalysts. Figure 3 shows the crystal morphology of MOF-199 and Ni-BTC at 5000x magnification. The results show that MOF-199 has an octahedral crystal shape. Synthesis at low temperatures generally produces cubic crystals with sharp edges, while at high temperatures, the shape is more rounded [34]. This study used a relatively low reaction temperature so that the resulting crystals had sharp edges. In Ni-BTC, the morphology and crystal structure characterized by FE-SEM shows that the resulting crystal structure is hexagonal, in accordance with research that has been reported [20]. The composition of MOF-199 according to EDX mapping data is 72.3% C, 20.1% O, and 7.7% Cu. As for Ni-BTC it is 55.8% C, 33.9% O, and 10.4%. More comprehensive EDX results can be seen in Figure S2 (Supporting Information).

The stability of the MOF can be observed from the characterization results with DTG. Figure 4(a) shows the decomposition of MOF-199. The results show that intensive weight loss occurs in two stages. First, at 25-180 °C, which refers to the loss of water and DMF, both adsorbed and coordinated with metal ions [25]. Second, at 270-450 °C, it is associated with the degradation of benzene tricarboxylic acid (BTC) as an organic linker and the collapse of the MOF structure, leaving CuO [33]. The Ni-BTC thermogram can be seen in Figure 4(b). At 25-110 °C, a weight loss of 2.4% represents a water loss. DMF loss was indicated by a weight loss of 23.16% at 110-250 °C. Furthermore, linker degradation occurs at 250-500 °C, and the MOF structure is damaged [27].

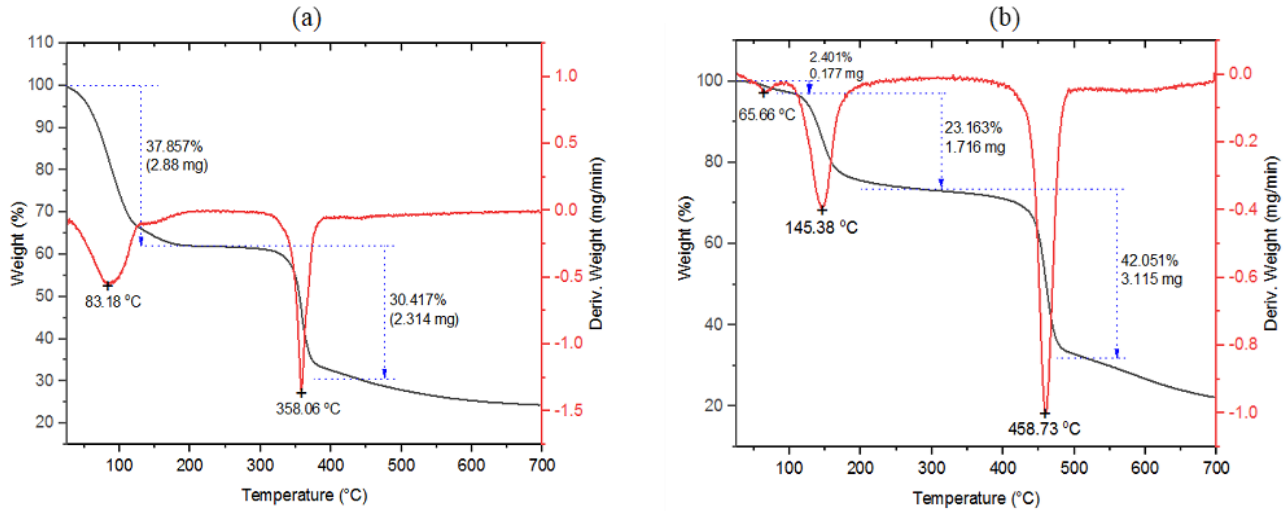

Figure 4. DTG curve of (a) MOF-199 and (b) Ni-BTC.

Copyright © 2023, ISSN 1978-2993

3.2 Catalytic Activity

MOF-199 and Ni-BTC were tested for their catalytic activity in 5-hydroxymethylfurfural (HMF) oxidation reaction to 2,5-furandicarboxylic acid (FDCA). The oxidation of HMF to FDCA can occur via two synthetic routes: The first is the formation of 2,5-diformylfuran (DFF) and/or 5-hydroxymethyl-2-furandicarboxylic acid (HMFCA). The conversion and the products were analyzed using HPLC. The peaks from the product are compared with the peaks of the standard solution. The results showed that FDCA, HMFCA, FFCA, HMF, and DFF peaks appeared at retention times of 8.05; 8.9; 9.6; 10.3; and 11.8 min (Figure S1 Supporting Information).

Product analysis results with HPLC can be seen in Figure 5. DFF peak did not appear, confirming that the formation of the synthetic pathway may not occur via DFF. On the other hand, the HMFCA and FFCA peaks were observed in small amounts. The HMF peak is very low, which indicates successful conversion to produce FDCA with the highest peak. No other peaks were observed as products, so MOF-199 and Ni-BTC had high selectivity.

FDCA yield, HMF conversion, and catalyst selectivity are shown in Figure 6. At 1 h, without catalyst, FDCA yield was below 10% and

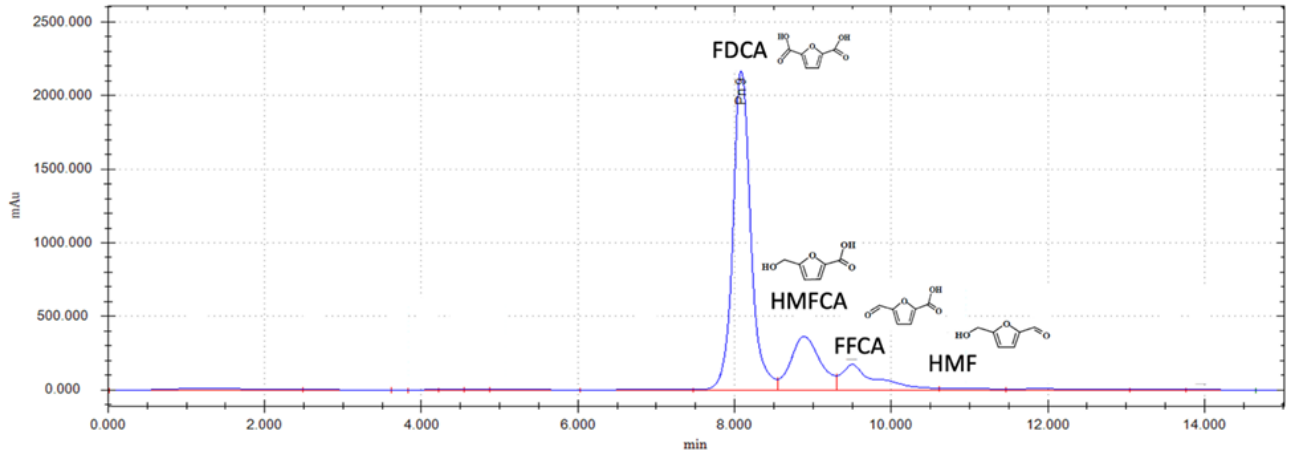

Figure 5. Product analysis results with HPLC.

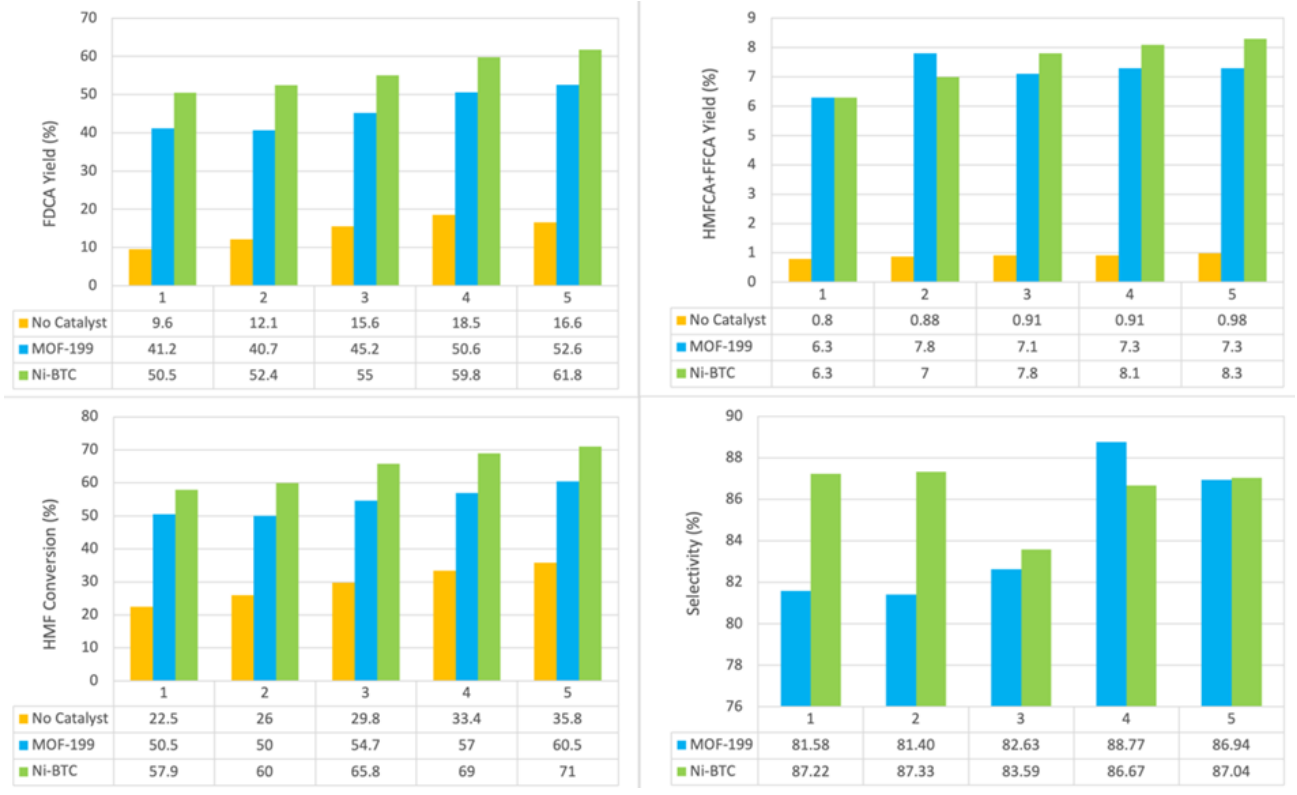

	1	2	3	4	5
No Catalyst	9.6	12.1	15.6	18.5	16.6
MOF-199	41.2	40.7	45.2	50.6	52.6
Ni-BTC	50.5	52.4	55	59.8	61.8

	1	2	3	4	5
No Catalyst	0.8	0.88	0.91	0.91	0.98
MOF-199	6.3	7.8	7.1	7.3	7.3
Ni-BTC	6.3	7	7.8	8.1	8.3

	1	2	3	4	5
No Catalyst	22.5	26	29.8	33.4	35.8
MOF-199	50.5	50	54.7	57	60.5
Ni-BTC	57.9	60	65.8	69	71

	1	2	3	4	5
MOF-199	81.58	81.40	82.63	88.77	86.94
Ni-BTC	87.22	87.33	83.59	86.67	87.04

Figure 6. Yield, conversion, and selectivity of HMF conversion into FDCA.

Copyright © 2023, ISSN 1978-2993

HMF conversion only 22.5%. FDCA yield increased up to 41 and 50.5% in the presence of MOF-199 and Ni-BTC. Similar results were obtained with the HMF conversion, which was 50.5 and 57.9%. At 2-4 h, no catalyst gave low results, while in the presence of the catalyst, FDCA yield and HMF conversion were improved, i.e., MOF-199 (40.7-50.6%; 50-57%) and Ni-BTC (52.4-59.8%; 60-69%). Finally, at 5 h, significant FDCA yield and HMF conversion were obtained for MOF-199 (52.6%; 60.5%) and Ni-BTC (61.8%; 71%). In contrast, at all reaction times, the side products of HMFCA and FFCA were negligible (less than 10%) and DFF was not detected. The selectivity of MOF-199 increased significantly with the length of the reaction time, where at 1 h, it was 81.58% to 86.94% after 5 h. Meanwhile, for Ni-BTC, changes in reaction time did not affect selectivity.

3.3 Proposed Reaction Mechanism

From product analysis using HPLC, it is known that the conversion of HMF to FDCA is only through by HMFCA formation reaction pathway without involving the formation of DFF. According to Zhou *et al.* [35], for HMF conversion reactions without DFF formation, there are two main phases in the overall oxidation process. In the first step, the hydroxide ion dissociates from the water, and the catalyst surface attracts the aldehyde side chain from the HMF. Aldehydes deposit hydroxide ions on the catalyst surface, which initiates a reversible hydration process that produces germinal diols. HMFCA is produced by oxidative dehydrogenation of the first intermediate diol, which desorbed the catalyst surface. In the second stage, CH− binds to the side chain of activated alcohol on the catalyst surface, forming an intermediate aldehyde that oxidizes further to produce FDCA just as in step 1. The oxidizing agent indirectly aids in the process by removing protons from the catalyst surface [36]. All reaction stages can occur due to the presence of metal bound to the O atom on the catalyst as observed from the results of IR spectra analysis (Figure 2). The presence of metals was also observed from the EDX analysis results (Figure S2 Supporting Information). The proposed reaction mechanism can be seen in Figure 7.

3.4 Correlation Between the Physicochemical Properties of the Catalyst and the Catalytic Activity

The catalytic activity of the catalyst is influenced by its physicochemical characteristics. In observing catalyst variations (Figure 6), heterogeneous catalysts play an essential role. The acidity of the catalyst has the most significant impact on catalytic activity, according to several characterizations that have been done. Figure 7 demonstrates that the Lewis acid on the catalyst surface contributes to the initial phases of the reaction. Ni-BTC has more acid sites than MOF-199, according to the results of the NH_3-TPD characterization (Figure 2(b)). Because of this, Ni-BTC has better catalytic activity. The number of coordinated metals in the MOF affects the number of Lewis acid sites. Ni-BTC has more coordinated Ni than Cu in MOF-199, according to EDX characterization (Figure 3).

From previous studies [24,37], Cu and Ni coordinated in MOF-199 and Ni-BTC are domi-

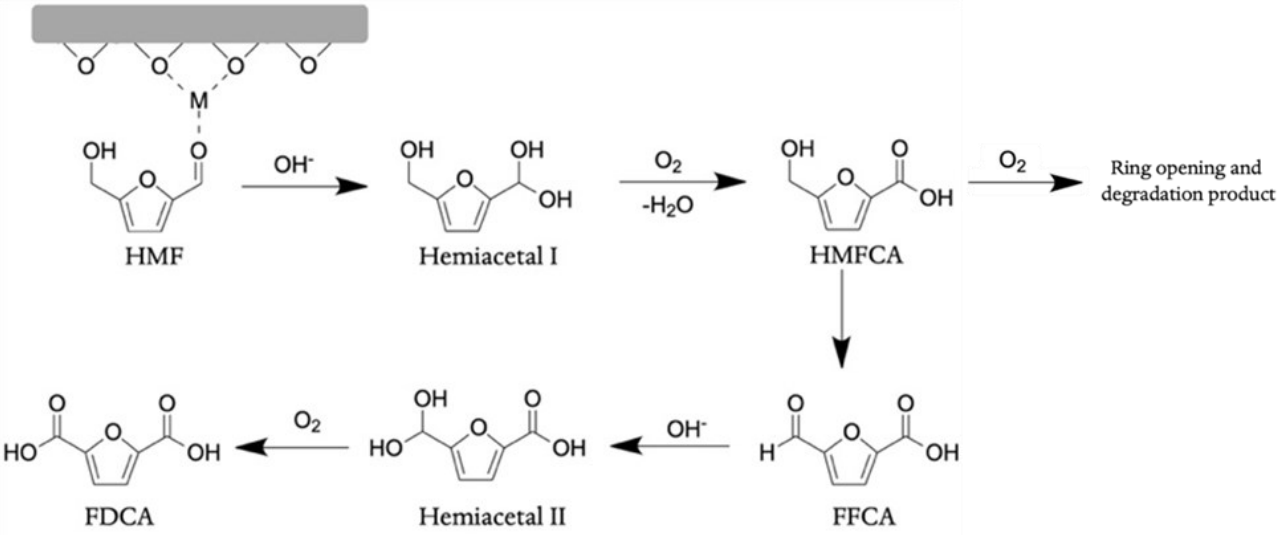

Figure 7. Proposed reaction mechanism.

Copyright © 2023, ISSN 1978-2993

nated by Cu^{2+} and Ni^{2+} which described the structure of MOF-199 and Ni-BTC. Ni^{2+} has moderate oxidizing ability, while Cu^{2+} is extremely high. The high oxidizing power of Cu^{2+} allows ring opening and product degradation (Figure 7) [38]. Moreover, compared to MOF-199, Ni-BTC is more temperature resistant. The thermogravimetric analysis results (Figure 4) serve as evidence for this.

4. Conclusions

MOF-199 and Ni-BTC has shown physicochemical properties that support its catalytic activity in HMF oxidation to FDCA. As-synthesized catalysts were a pure phase with no obvious peaks of impurities and crystal structure was octahedral and hexagonal shape for MOF-199 and Ni-BTC, respectively. The best catalytic activity was given by Ni-BTC with 71% of HMF conversion, 61.8% of FDCA yield, and 87% of selectivity due to the higher acid content compared with MOF-199. The longer the reaction time, the greater the FDCA yield with the optimum time being 5 h.

Acknowledgment

This research was funded by Indonesia Ministry of Education, Culture, Research, and Technology under PDD 2023 Grant (Grant No. NKB-978/UN2.RST/HKP.05.00/2022).

CRediT Authors Statement

Author Contributions: *I. Herlina*: Investigation, Formal Analysis, Writing- Reviewing and Editing; *Y. K. Krisnandi*: Conceptualization, Methodology, Supervision, Funding acquisition, Writing-Reviewing and Editing; *M. Ridwan*: Conceptualization, Methodology, Supervision, Reviewing. All authors have read and agreed to the published version of the manuscript.

References

[1] Al-Hamamre, Z., Saidan, M., Hararah, M., Rawajfeh, K., Alkhasawneh, H.E., Al-Shannag, M. (2017). Wastes and biomass materials as sustainable-renewable energy resources for Jordan. *Renewable and Sustainable Energy Reviews*, 67, 295–314. DOI: 10.1016/j.rser.2016.09.035.

[2] Salanti, A., Zoia, L., Orlandi, M., Zanini, F., Elegir, G. (2010). Structural characterization and antioxidant activity evaluation of lignins from rice husk. *Journal of Agricultural and Food Chemistry*, 58(18), 10049–10055. DOI: 10.1021/jf102188k.

[3] Jiang, Z., Zeng, Y., Hu, D., Guo, R., Yan, K., Luque, R. (2022). Chemical transformations of 5-hydroxymethylfurfural into highly added value products: present and future. *Green Chemistry*, 25(3), 871–892. DOI: 10.1039/d2gc03444a.

[4] Tong, X., Ma, Y., Li, Y. (2010). Biomass into chemicals: Conversion of sugars to furan derivatives by catalytic processes. *Applied Catalysis A: General*, 385(1–2), 1–13. DOI: 10.1016/j.apcata.2010.06.049.

[5] Saebea, D., Soisuwat, S., Arpornwichanop, A., Patcharavorachot, Y. (2023). Simulation-based Assessment of 2,5 Furandicarboxylic Acid Production from Oxidation of 5-Hydroxymethylfurfural. *Chemical Engineering Transactions*, 98, 87–92. DOI: 10.3303/CET2398015.

[6] Gomes, M., Gandini, A., Silvestre, A.J.D., Reis, B. (2011). Synthesis and characterization of poly(2,5-furan dicarboxylate)s based on a variety of diols. *Journal of Polymer Science, Part A: Polymer Chemistry*, 49(17), 3759–3768. DOI: 10.1002/pola.24812.

[7] De Jong, E., Dam, M.A., Sipos, L., Gruter, G.J.M. (2012). Furandicarboxylic acid (FDCA), A versatile building block for a very interesting class of polyesters. *ACS Symposium Series*, 1105, 1–13. DOI: 10.1021/bk-2012-1105.ch001.

[8] Rose, M., Weber, D., Lotsch, B. V, Kremer, R.K., Goddard, R., Palkovits, R. (2013). Biogenic metal-organic frameworks: 2,5-Furandicarboxylic acid as versatile building block. *Microporous and Mesoporous Materials*, 181, 217–221. DOI: 10.1016/j.micromeso.2013.06.039.

[9] Hayashi, E., Komanoya, T., Kamata, K., Hara, M. (2017). Heterogeneously-Catalyzed Aerobic Oxidation of 5-Hydroxymethylfurfural to 2,5-Furandicarboxylic Acid with MnO2. *ChemSusChem*, 10(4), 654–658. DOI: 10.1002/cssc.201601443.

[10] Megías-Sayago, C., Lolli, A., Bonincontro, D., Penkova, A., Albonetti, S., Cavani, F., Odriozola, J.A., Ivanova, S. (2020). Effect of Gold Particles Size over Au/C Catalyst Selectivity in HMF Oxidation Reaction. *ChemCatChem*, 12(4), 1177–1183. DOI: 10.1002/cctc.201901742.

[11] Ahmed, M.S., Mannel, D.S., Root, T.W., Stahl, S.S. (2017). Aerobic Oxidation of Diverse Primary Alcohols to Carboxylic Acids with a Heterogeneous Pd-Bi-Te/C (PBT/C) Catalyst. *Organic Process Research and Development*, 21(9), 1388–1393. DOI: 10.1021/acs.oprd.7b00223.

Copyright © 2023, ISSN 1978-2993

[12] Gong, W., Zheng, K., Ji, P. (2017). Platinum deposited on cerium coordination polymer for catalytic oxidation of hydroxymethylfurfural producing 2,5-furandicarboxylic acid. *RSC Advances*, 7(55), 34776–34782. DOI: 10.1039/c7ra05427k.

[13] Kucherov, F.A., Romashov, L. V, Galkin, K.I., Ananikov, V.P. (2018). Chemical Transformations of Biomass-Derived C6-Furanic Platform Chemicals for Sustainable Energy Research, Materials Science, and Synthetic Building Blocks. *ACS Sustainable Chemistry and Engineering*, 6(7), 8064–8092. DOI: 10.1021/acssuschemeng.8b00971.

[14] Stöcker, M. (2008). Biofuels and biomass-to-liquid fuels in the biorefinery: Catalytic conversion of lignocellulosic biomass using porous materials. *Angewandte Chemie - International Edition*, 47(48), 9200–9211. DOI: 10.1002/anie.200801476.

[15] Furukawa, H., Cordova, K.E., O'Keeffe, M., Yaghi, O.M. (2013). The chemistry and applications of metal-organic frameworks. *Science*, 341(6149), 1230444. DOI: 10.1126/science.1230444.

[16] Liao, Y. Te, Nguyen, V.C., Ishiguro, N., Young, A.P., Tsung, C.K., Wu, K.C.-W. (2020). Engineering a homogeneous alloy-oxide interface derived from metal-organic frameworks for selective oxidation of 5-hydroxymethylfurfural to 2,5-furandicarboxylic acid. *Applied Catalysis B: Environmental*, 270, 118805. DOI: 10.1016/j.apcatb.2020.118805.

[17] Chui, S.S.-Y., Lo, S.M.-F., Charmant, J.P.H., Orpen, A.G., Williams, I.D. (1999). A chemically functionalizable nanoporous material [$Cu_3(TMA)_2(H_2O)_3$](n). *Science*, 283(5405), 1148–1150. DOI: 10.1126/science.283.5405.1148.

[18] Sarwar, E., Noor, T., Iqbal, N., Mehmood, Y., Ahmed, S., Mehek, R. (2018). Effect of Co-Ni Ratio in Graphene Based Bimetallic Electrocatalyst for Methanol Oxidation. *Fuel Cells*, 18(2), 189–194. DOI: 10.1002/fuce.201700143.

[19] Thi, T.V.N., Luu, C.L., Hoang, T.C., Nguyen, T., Bui, T.H., Nguyen, P.H.D., Thi, T.P.P. (2013). Synthesis of MOF-199 and application to CO_2 adsorption. *Advances in Natural Sciences: Nanoscience and Nanotechnology*, 4(3), 35016. DOI: 10.1088/2043-6262/4/3/035016.

[20] Yaqoob, L., Noor, T., Iqbal, N., Nasir, H., Zaman, N. (2019). Development of nickel-BTC-MOF-derived nanocomposites with rGO towards electrocatalytic oxidation of methanol and its product analysis. *Catalysts*, 9(10), 856. DOI: 10.3390/catal9100856.

[21] Israr, F., Kim, D.K., Kim, Y., Chun, W. (2016). Scope of various solvents and their effects on solvothermal synthesis of Ni-BTC. *Quimica Nova*, 39 (6), 669–675. DOI: 10.5935/0100-4042.20160068.

[22] Ediati, R., Kahardian, M., Hartanto, D. (2016). Pengaruh Perbandingan Pelarut Etanol dan Dimetilformamida pada Sintesis Metal Organik Framework HKUST-1. *Akta Kimia Indonesia*, 1 (1), 25–33. DOI: 10.12962/j25493736.v1i1.1425.

[23] Kumar, R.S., Kumar, S.S., Kulandainathan, M.A. (2013). Efficient electrosynthesis of highly active Cu_3(BTC) 2-MOF and its catalytic application to chemical reduction. *Microporous and Mesoporous Materials*, 168, 57–64. DOI: 10.1016/j.micromeso.2012.09.028.

[24] Li, L., Liu, X.L., Geng, H.Y., Hu, B., Song, G.W., Xu, Z.S. (2013). A MOF/graphite oxide hybrid (MOF: HKUST-1) material for the adsorption of methylene blue from aqueous solution. *Journal of Materials Chemistry A*, 1(35), 10292–10299. DOI: 10.1039/c3ta11478c.

[25] Mahmoodi, N.M., Abdi, J. (2019). Nanoporous metal-organic framework (MOF-199): Synthesis, characterization and photocatalytic degradation of Basic Blue 41. *Microchemical Journal*, 144, 436–442. DOI: 10.1016/j.microc.2018.09.033.

[26] Chen, B., Zhao, X., Putkham, A., Hong, K., Lobkovsky, E.B., Hurtado, E.J., Fletcher, A.J., Thomas, K.M. (2008). Surface interactions and quantum kinetic molecular sieving for H2 and D2 adsorption on a mixed metal-organic framework material. *Journal of the American Chemical Society*, 130(20), 6411–6423. DOI: 10.1021/ja710144k.

[27] Israr, F., Chun, D., Kim, Y., Kim, D.K. (2016). High yield synthesis of Ni-BTC metal-organic framework with ultrasonic irradiation: Role of polar aprotic DMF solvent. *Ultrasonics Sonochemistry*, 31, 93–101. DOI: 10.1016/j.ultsonch.2015.12.007.

[28] Sanaei, M., Fazaeli, R., Aliyan, H. (2019). Pd/MOF-199: As an efficient heterogeneous catalyst for the Suzukie Miyaura cross-coupling reaction. *Journal of the Chinese Chemical Society*, 66(10), 1290–1295. DOI: 10.1002/jccs.201800428.

[29] Gao, W.Y., Leng, K., Cash, L., Chrzanowski, M., Stackhouse, C.A., Sun, Y., Ma, S. (2015). Investigation of prototypal MOFs consisting of polyhedral cages with accessible Lewis-acid sites for quinoline synthesis. *Chemical Communications*, 51(23), 4827–4829. DOI: 10.1039/c4cc09410g.

Copyright © 2023, ISSN 1978-2993

[30] Chowdhury, P., Bikkina, C., Meister, D., Dreisbach, F., Gumma, S. (2009). Comparison of adsorption isotherms on Cu-BTC metal organic frameworks synthesized from different routes. *Microporous and Mesoporous Materials*, 117 (1–2), 406–413. DOI: 10.1016/j.micromeso.2008.07.029.

[31] Li, C., Zheng, M., Wang, A., Zhang, T. (2012). One-pot catalytic hydrocracking of raw woody biomass into chemicals over supported carbide catalysts: Simultaneous conversion of cellulose, hemicellulose and lignin. *Energy and Environmental Science*, 5 (4), 6383–6390. DOI: 10.1039/c1ee02684d.

[32] Xue, Z., Zhang, J., Peng, L., Han, B., Mu, T., Li, J., Yang, G. (2014). Poly(ethylene glycol) stabilized mesoporous metal-organic framework nanocrystals: Efficient and durable catalysts for the oxidation of benzyl alcohol. *ChemPhysChem*, 15 (1), 85–89. DOI: 10.1002/cphc.201300809.

[33] Sun, B., Kayal, S., Chakraborty, A. (2014). Study of HKUST (Copper benzene-1,3,5-tricarboxylate, Cu-BTC MOF)-1 metal organic frameworks for CH4 adsorption: An experimental Investigation with GCMC (grand canonical Monte-carlo) simulation. *Energy*, 76, 419–427. DOI: 10.1016/j.energy.2014.08.033.

[34] Wang, Q.M., Shen, D., Bülow, M., Lau, M.L., Deng, S., Fitch, F.R., Lemcoff, N.O., Semanscin, J. (2002). Metallo-organic molecular sieve for gas separation and purification. *Microporous and Mesoporous Materials*, 55(2), 217–230. DOI: 10.1016/S1387-1811(02)00405-5.

[35] Zhou, H., Xu, H., Liu, Y. (2019). Aerobic oxidation of 5-hydroxymethylfurfural to 2,5-furandicarboxylic acid over Co/Mn-lignin coordination complexes-derived catalysts. *Applied Catalysis B: Environmental*, 244, 965–973. DOI: 10.1016/j.apcatb.2018.12.046.

[36] Su, H., Zhang, K.X., Zhang, B., Wang, H.H., Yu, Q.Y., Li, X.H., Antonietti, M., Chen, J.S. (2017). Activating cobalt nanoparticles via the Mott-Schottky effect in nitrogen-rich carbon shells for base-free aerobic oxidation of alcohols to esters. *Journal of the American Chemical Society*, 139 (2), 811–818. DOI: 10.1021/jacs.6b10710.

[37] Oliveira, H., Scacchetti, F., Bezerra, F., Santos, J., Soares, G. (2023). Comprehensive evaluation of HKUST-1 as an efficient adsorbent for textile dyes. *Environmental Science and Pollution Research*, 30 (37), 87242–87259. DOI: 10.1007/s11356-023-28455-3.

[38] Sajid, M., Zhao, X., Liu, D. (2018). Production of 2,5-furandicarboxylic acid (FDCA) from 5-hydroxymethylfurfural (HMF): Recent progress focusing on the chemical-catalytic routes. *Green Chemistry*, 20 (24), 5427–5453. DOI: 10.1039/c8gc02680g.

Please see other information in the separated Supporting Information (SI).

Copyright © 2023, ISSN 1978-2993